Coordination-number-induced morphological structural transition in a network glass

B. Norban, D. Pershing, R. N. Enzweiler, and P. Boolchand
University of Cincinnati, Cincinnati, Ohio 45221-0030

J. E. Griffiths and J. C. Phillips
AT&T Bell Laboratories, Murray Hill, New Jersey 07974

(Received 14 November 1986; revised manuscript received 9 July 1987)

Mössbauer electric field gradients, Raman vibrational modes, and crystallization temperatures exhibit threshold behavior near the composition $x=0.20$ in binary Si_xTe_{1-x} glasses. This threshold is evidence of a morphological structural change that may be driven by network connectivity or average coordination number. At $x \leq 0.20$, the network largely consists of Si-cross-linked Te_n chain segments. At $x \geq 0.20$, Te_n chains reconstruct with tetrahedral $Si(Te_{1/2})_4$ units and nucleate a defect-ridden Si_2Te_3-like layered molecular fragment. These fragments represent the elastically rigid domains that percolate above the threshold.

I. INTRODUCTION

Current interest in elastic properties of glassy networks has been stimulated by the idea of rigidity percolation.[1,2] Undercoordinated (or underconstrained) networks corresponding to a mean coordination number $\langle m \rangle < 2.40$ are pictured as elastically floppy because these networks are easily deformed under a shearing force. On the other hand, overcoordinated (or overconstrained) networks corresponding to $\langle m \rangle > 2.40$ are visualized as elastically rigid because such networks resist a change in shape under a shearing force. These ideas due to Phillips[1] and Thorpe[2] have led to the realization that at the threshold coordination number of $\langle m \rangle = 2.40$, a glass network constrained by bond-stretching and -bending forces sits at a mechanical critical point in which rigid regions are thought to percolate in a mean-field sense. In a glassy A_xB_{1-x} network composed of cations (A=Ge,Si) and anions (B=S, Se, and Te) that are, respectively, fourfold and twofold coordinated, the critical composition $x=x_c$ corresponding to vector percolation is given by

$$2(x_c+1)=2.40$$

yielding $x_c=0.20$. Experimental evidence in support of mechanical thresholds in binary Ge-Se (Ref. 3) glasses and ternary Ge-As-Se glasses[4] was recently provided using a macroscopic probe (ultrasonic elastic constant) of network rigidity. The structural consequences of mechanical thresholds were elucidated by Bresser *et al.* using Mössbauer site spectroscopy[5] which was also correlated with Raman band spectroscopy.[6]

In this paper we present experimental evidence for thresholds in ^{125}Te electric field gradients, Raman vibrational modes, and crystallization temperatures each occurring very near the composition $x=0.20$ in binary Si_xTe_{1-x} glasses. These results appear to be consistent with the notion that molecular fragments based on the c-Si_2Te_3 structure are populated in the bulk glasses above the vector percolation threshold at $x \geq 0.20$. At $x \leq 0.20$ Te_n chain segments and tetrahedral $Si(Te_{1/2})_4$ units predominantly occur in the glassy networks. The present experiments, along with those reported[3-6] recently, appear to demonstrate that the so-called mechanically rigid regions present in overcoordinated glasses largely consist of compacted molecular fragments derived from corresponding crystals.

II. EXPERIMENTAL PROCEDURES

Binary Si_xTe_{1-x} glasses were prepared by alloying the elements in vacuum followed by a water quench. 99.9999%-pure Si chunks and 99.9999%-pure Te chunks from Cerac Inc., Milwaukee, Wisconsin, were used as the starting materials. The elements in the desired proportion were sealed in 5-mm-inner-diameter fused-quartz ampules at a pressure of 5×10^{-7} Torr using a CTI cryopump-based vacuum system. The melts, typically 0.5 g in size, were held at 1000 °C for 5 d in a vertical configuration and periodically shaken to homogenize before quenching in water. This procedure yielded homogeneous glassy samples in the composition range $0.10<x<0.25$ that displayed reproducible glass transition $T_g(x)$ and crystallization temperatures $T_c(x)$.

Our differential-scanning-calorimetry traces taken with a Perkin-Elmer model 2C instrument at selected compositions x are displayed in Fig. 1. These results show the presence of two distinct crystallization temperatures, T_{c1} and T_{c2} at $x \leq 0.20$ but only one crystallization temperature at $x \geq 0.21$. Figure 2 displays the compositional dependence of $T_g(x)$, $T_{c1}(x)$, and $T_{c2}(x)$ taken at a 20-K/min scan rate.

Raman scattering from the bulk glass chips was obtained using the 7525-Å exciting line from a Kr-ion laser. Spectra were recorded as a function of laser power to understand the various steps leading to photocrystallization both at $x<0.20$ and at $x>0.20$. Details of the experimental setup are described elsewhere.[7] Figures 3(a) and 3(b) reproduce spectra observed at $x=0.18$

and 0.23. Reference spectra of the crystals in this binary compound (*c*-Te and *c*-Si_2Te_3) were also obtained for purposes of comparison.

^{125}Te Mössbauer spectra of the glasses were taken at 4.2 K using a source of half-life 58 d, $^{125}Te^m$ in cubic GeTe.[8] The spectra of the glasses display a quadrupole doublet whose splitting (Δ) decreases with x in a systematic fashion to display a cusp at $x=0.20$ shown in Fig. 4. The spectrum of *c*-Si_2Te_3 was also studied for reference purposes. ^{129}I emission spectra of the glasses and of *c*-Si_2Te_3 were also studied and will be discussed elsewhere.

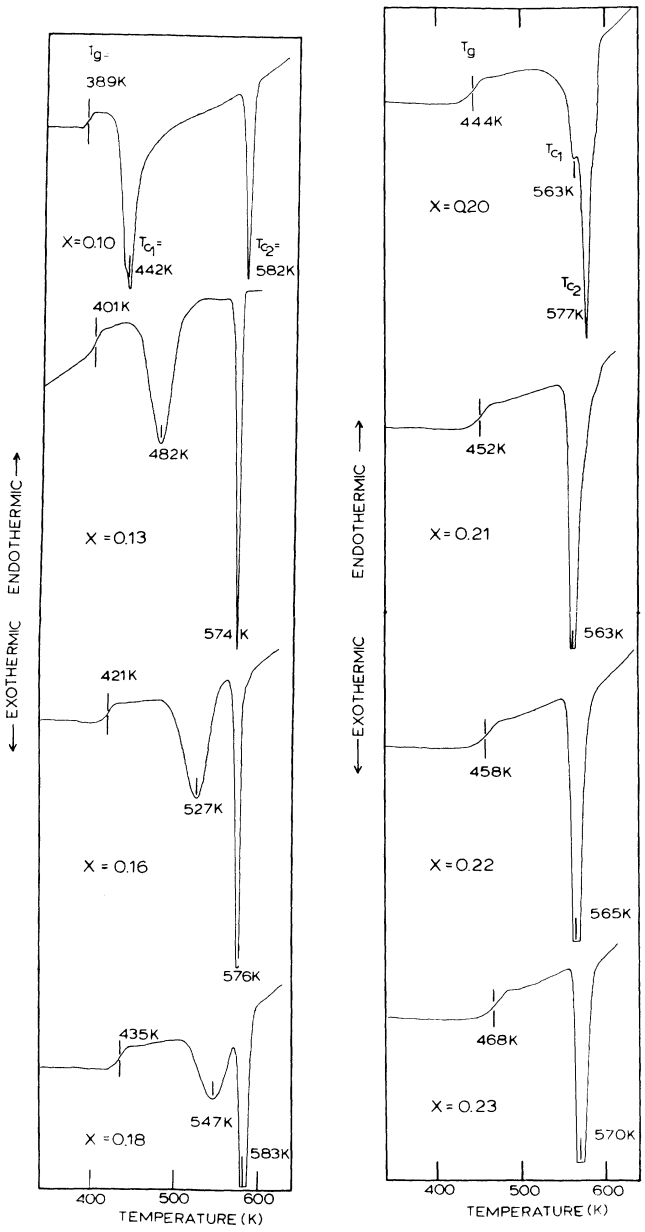

FIG. 1. Differential scanning calorimetry results on Si_xTe_{1-x} glasses plotted as a function of x. A scan rate of 20 K/min, a range setting of 5, and $\sim$20 mg mass of the glass sample were used to obtain these scans on a Perkin-Elmer model 2C instrument.

III. DISCUSSION OF RESULTS AND GLASS MOLECULAR STRUCTURE

The glass-structure consequences of our calorimetric and spectroscopic results are discussed sequentially in this section.

A. Differential scanning calorimetry

Several years ago Cornet[9] found that the compositional dependence of glass transition temperatures $T_g(x)$ and first crystallization temperatures $T_{c1}(x)$ in binary Si_xTe_{1-x} glasses is linear in the composition range $0.10 \leq x \leq 0.25$. Our results confirm the linear variation of $T_g(x)$ and $T_{c1}(x)$ found earlier by Cornet. These results do differ qualitatively from those of Asokan, Parthasarathy, and Gopal,[10] however, who observe a local minimum in both $T_g(x)$ and $T_{c1}(x)$ at $x=0.20$. The difference between our results and those of Asokan *et al.* are probably related to different sample-preparation conditions and will be discussed elsewhere.

Particularly noteworthy in our scans is the existence of two crystallization temperatures T_{c1} and T_{c2} at $x \lesssim 0.21$ but only one crystallization exotherm at $x \gtrsim 0.21$. Similar homogeneous behavior in crystallization temperatures of these glasses above the threshold composition x_c is also observed by Asokan *et al.* on their samples.[10] We have also carried out these calorimetric experiments at a much smaller scan rate of 5 K/min and find that the threshold composition of $x_c \simeq 0.20$ is not altered although the absolute values of T_{c1} and T_{c2} are systematically lowered. Clearly the existence of the threshold composition $x_c=0.20$ is not a

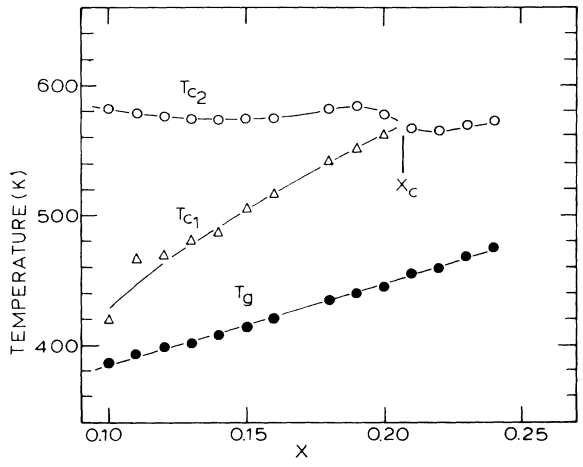

FIG. 2. Glass transition temperatures $T_g(x)$, first crystallization temperatures $T_{c1}(x)$, and second crystallization temperatures $T_{c2}(x)$ in binary Si_xTe_{1-x} glasses plotted as a function of x. Note that at $x=x_c \simeq 0.21$ T_{c1} and T_{c2} coalesce and at $x \geq 0.21$ only one crystallization temperature is observed. The linear variation of $T_g(x)$ is signature of molecular phase separation of the glassy networks as discussed in text.

kinetic phenomenon associated with the crystallization process but must have a structural origin.

We identify the temperature T_{c1} with crystallization of the "floppy part" of the glass network, i.e., amorphous Te, to form c-Te, while the temperature T_{c2} is associated with crystallization of the rigid Si-containing cross links to form c-Si_2Te_3. The floppiness of the amorphous Te network derives from both chemical as well as topological considerations. The former is due to the large mass of the Te atoms ($m_{Te}=127$) relative to silicon ($m_{Si}=28$) producing very soft Te—Te covalent bonds and, therefore, a low melting point. The low coordination number of Te ($m=2$) on the other hand represents the topological factor contributing to the floppiness of the amorphous Te network. The first step toward crystallization of Te-rich binary $Te_{1-x}Z_x$ glasses (Z=Si, Ge, Al, Ga, . . .) is the splitting off[9,10] of trigonal Te_n chains leaving a glass residue that is enriched in Z and understandably is characterized[10] by a higher T_g than the virgin glass. Above the threshold, i.e., $x \geq 0.20$, the occurrence of a unique crystallization temperature may be explained by the coalescing of the $Si(Te_{1/2})_4$ units with the excess Te (in the chain fragments) to nucleate a new rigid molecular fragment based on close-packed layers of Te in which Si_2 units are inserted. The linear variation of $T_g(x)$ observed in the present glasses is quite similar to a variation reported earlier in As-S (Ref. 11) and Ge-Sn-S glasses.[12] These results are consistent with the idea that phase separation of these glassy networks intrinsically occurs on a scale characteristic of large molecules.

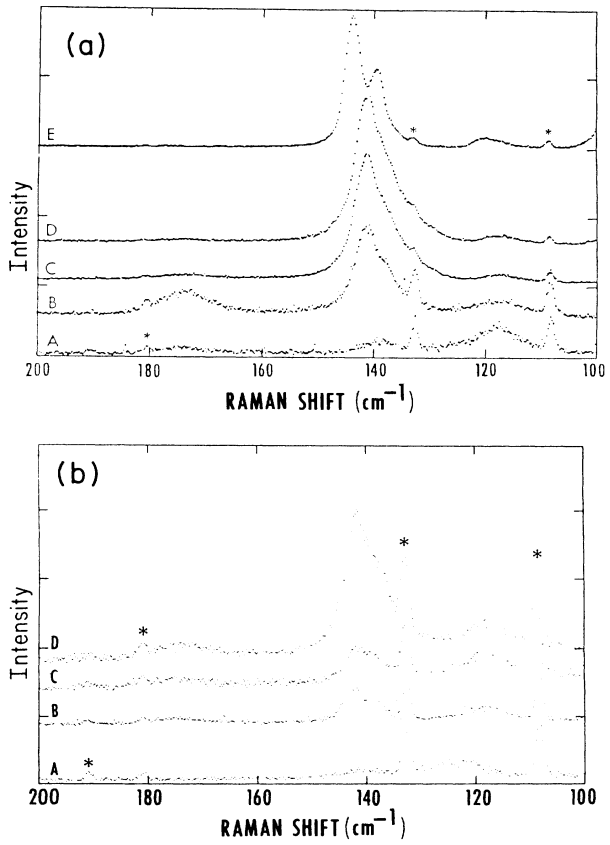

FIG. 3. (a) Raman spectra of $Si_{18}Te_{82}$ as a function of laser power in mW at 7525 A: A, 21; B, 32; C, 45; D; 64; E, 10. Power was reduced to 10 mW for 30 min after D before scanning to record E. Asterisks indicate laser plasma lines. Spectra are offset for clarity. Experimental parameters are 0.25 cm^{-1}/step, 10 sec counting time per step, spectral slit width, 1.2 cm^{-1}. The amplitudes of the most intense peaks in A-E vary. They are 3000 counts/sec in E and 18 counts/sec in A. (b) Raman spectra of $Si_{23}Te_{77}$ as a function of laser power in mW at 7525 A: A, 6.4; B, 16; C, 19.3; D, 28.5. Asterisks indicate laser plasma lines. All other parameters are the same as in 3(a).

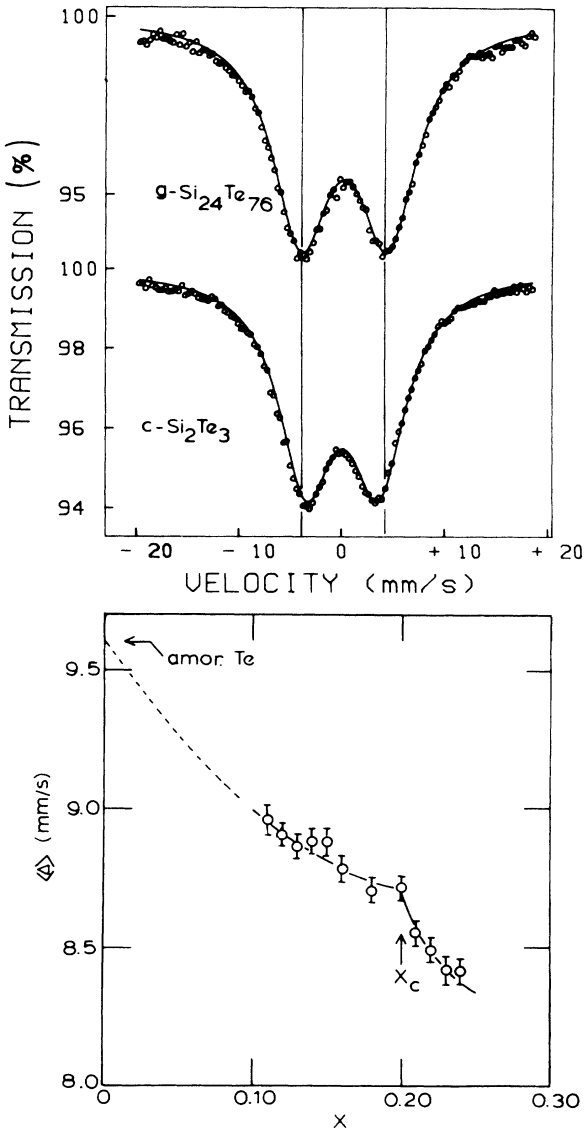

FIG. 4. ^{125}Te Mössbauer spectra of indicated glass and crystal recorded at 4.2 K using a source of $^{125}Te^m$ in c-GeTe. The quadrupole splitting (Δ) of g-$Si_{24}Te_{76}$ and c-Si_2Te_3 are 8.4 and 7.1 mm/s. The lower panel shows the x variation of Δ in the glasses exhibiting a cusp near $x=0.20$. See text for details.

Support for such a picture can be found in our spectroscopic results which we discuss next.

B. Raman scattering

Our Raman scattering results on $Si_{18}Te_{82}$ glass [Fig. 3(a)] at the lowest power (spectrum A, 21 mW) display three broad peaks at 118, 138, and 173 cm^{-1}. The lowest-frequency modes can be attributed[13] to disordered chains of Te which are either phase separated by photoinduced bond cleavage or are connected at one end of each chain to structural elements existing in the glass. Analogous phonon frequencies for ordered chains (Te_n) in c-Te are known[13] to occur at 123 and 143 cm^{-1}. Dramatic changes begin to evolve at higher powers ($B-D$). The peak at 173 cm^{-1} rapidly grows in strength in B and almost completely disappears by D. Simultaneously, a very intense peak of complex band shape continues to grow from B through D with peak frequency of about 141 cm^{-1}. These changes appear to indicate the existence of $SiTe_3$ face-sharing tetrahedra emerging in the glasses. Such tetrahedra are known to occur in c-Si_2Te_3.[14] One also notes that the nature of the peak near 120 cm^{-1} changes its position and shape as the bulk glass in the scattering volume evolves toward a Si_2Te_3 composition.

Several comments can be made on the microscopic origin of the 173-cm^{-1} mode. This mode does not arise from elemental Te nor is it observed in the spectrum of c-Si_2Te_3. A reasonable candidate is clusters composed of $SiTe_{4/2}$ tetrahedral units which intrinsically occur in the virgin glass as revealed by the presence of this band in spectrum A. Laser irradiation at a 32-mW power level (spectrum B, Fig. 3) significantly enhances the signal strength of the 173-cm^{-1} band probably because cleaving of Te_n chains blue-shifts the optical-absorption edge and leaves a Si-rich bulk glass in which metastable clusters of tetrahedral $SiTe_{4/2}$ units predominate. At still higher power level, these clusters reconstruct with the cleaved Te_n chains to nucleate Si_2Te_3 crystals which display[15] the narrow but intense band at 145 cm^{-1}. These results also show the metastable character of the $SiTe_{4/2}$ units present in the glass. Such tetrahedral units apparently do not occur in a crystalline form as revealed by the absence of a stable crystalline compound of $SiTe_2$ stoichiometry.[14]

One may estimate the expected peak vibrational frequencies of possible $SiTe_{4/2}$ structural units by analogy with the frequencies of similar structural entities in SiS_2 and $SiSe_2$ glasses and in Si_xS_{1-x} and Si_xSe_{1-x} nonstoichiometric glasses.[17] The structural units are face-sharing tetrahedra in silicon-rich nonstoichiometric glasses, and both corner-sharing and edge-sharing tetrahedra in the stoichiometric SiS_2 and $SiSe_2$ glasses. To factor out the reduced mass effect on the frequencies on going from the sulfides to the selenides to the tellurides each observed frequency is scaled to the appropriate ν_1 frequency of $SiCl_4$, $SiBr_4$, or SiI_4 molecules. For example, the frequency associated with the symmetric ν_1 mode of a face-sharing tetrahedron in $SiSe_2$ glass occurs at 200 cm^{-1}. The ratio of this frequency to the ν_1 mode at 247 cm^{-1} in $SiBr_4$ is 0.81. For $SiSi_2$, one uses the 333-cm^{-1} peak frequency of the face-sharing mode and the 424-cm^{-1} ν_1 frequency of $SiCl_4$ to give $333/424=0.79$, a value very close to the 0.81 value determined for SiS_2. Thus, one might expect a similar value for $SiTe_{4/2}$ face-sharing tetrahedra. A summary of such considerations is given in Table I. From these calculations, the observed band at 173 cm^{-1} in the Si-Te glasses would appear to arise from a stretching mode localized in edge-sharing tetrahedra. Correspondingly, the band observed at 141 cm^{-1} appears to be associated with vibrational motions in face-sharing tetrahedra.

After spectrum D was recorded at a power level of 64 mW, the incident power was reduced to 10 mW for 30 min before scanning E at that power. This significantly reduces the optical and thermal energy input to the sample and allows cooling and crystallization to occur with the formation of c-Si_2Te_3 as is evident in E. The scattering cross section of Si_2Te_3 is so large compared to other species that it dominates the observed spectrum. In the dark, over a period of 17 h at room temperature, crystallization is partially reversed but the spectrum of c-Si_2Te_3 can still be observed. Its intensity relative to E is reduced by a factor of about 50. The surface of the sample, however, has suffered observable damage. Melting is indicated and is consistent with the observations in spectra D and E.

Samples with $x>0.20$ behave under the influence of laser irradiation in much the same way as those with $x<0.20$ with one main exception. The amplitude of the 173-cm^{-1} band is much diminished and as the Si to Te ratio increases, it plays a lesser and lesser role in the convoluted pathway toward crystallization [Fig. 3(b)]. This supports our previous inference that the molecular structure responsible for this band has a composition $x<0.4$. It is striking that this transitional band appears most strongly for x close to $x=0.18$ which is close to $x_c=0.20$. Samples with $x=0.18\pm0.02$ show this band more strongly than for samples with $x=0.23$. The structure responsible for this band forms just before x increases to x_c, and may be a precursor to defective Si_2Te_3.

C. Mössbauer spectroscopy

^{125}Te Mössbauer spectra of the binary glasses display a partially resolved doublet (upper panel of Fig. 4) whose origin is traced[18] to a nuclear quadrupole splitting (Δ) in the $\frac{3}{2}+$ first excited state. The quadrupole splitting measures the electric field gradient, which in these covalent materials is determined principally by the distribution of electrons in the $5p$ bonding and nonbonding lone pairs of Te at various sites in the network.[19] Since the natural linewidth of the ^{125}Te resonance of 5.20 mm/s is comparable to the quadrupole splittings (~ 8 mm/s) of the Te sites, it is not possible to unambiguously deconvolute contributions of the chemically inequivalent Te sites from the spectra. However, we have succeeded in deconvoluting contributions of at least two types of Te sites in these glasses using ^{129}I emission spec-

TABLE I. Structure-element frequency calculations.

Structural elements	ν_1 (cm^{-1})[a]	$\nu_1(SiS_2)/\nu_1(SiCl_4)$	ν_1 (cm^{-1})[b]	$\nu_1(SiSe_2)/\nu_1(SiBr_4)$	ν_1 (cm^{-1})[c]	$\nu_1(SiTe_2)/\nu_1(SiI_4)$
Face sharing	333[d]	0.79	200	0.81	141	0.85
Corner sharing	381	0.90	227	0.92		
Edge sharing	427	1.01	245	0.99	173	1.04

[a]Reference 16.
[b]Reference 17.
[c]This work.
[d]Data from (a) are interpreted in terms of the recent structural model of (b).

troscopy, the results of which are discussed elsewhere. The two sites in question are as follows. One of these sites (site B) represents a Te site that is twofold coordinated to Te near neighbors in a Te chain segment as in *a*-Te. This site possesses a large $\Delta_B = 9.6$ mm/s as shown elsewhere.[18,19] The second site (site A) represents a Te site that is twofold coordinated to Si near neighbors and this site acts as a bridge between tetrahedral $Si(Te_{1/2})_4$ units, with a smaller $\Delta_A \simeq 7.3$ mm/s.

Starting from *a*-Te (i.e., $x=0$), we can understand the decline in $\langle \Delta(x) \rangle$ in the composition range $0 \leq x \leq 0.20$ in terms of growth in the Te A-site population at the expense of Te B sites, as progressive Si alloying promotes crosslinking of the Te chain segments. The more rapid decline in $\langle \Delta(x) \rangle$ at $x \geq 0.20$ which leads to the cusp at $x=0.20$ is signature of more drastic structural changes taking place in the glass network at the mechanical threshold. We can understand the sharp reduction in $\langle \Delta \rangle$ due to a sudden loss in the Te chain sites as the Te chain segments rapidly coalesce with the tetrahedral $Si(Te_{1/2})_4$ units at $x \gtrsim 0.20$ to nucleate a new molecular fragment. This fragment consists of close-packed layers of Te atoms based on the defect-ridden Si_2Te_3-like layered cluster in which instead of the usual $\frac{1}{3}$ Si dimer vacancies, there are more like $\frac{2}{3}$ vacancies corresponding to a stoichiometry of $SiTe_3$ appropriate for $x \simeq 0.25$. On chemical grounds this reconstruction appears plausible for several reasons.[14,20] X-ray crystallographic studies of Gregoriades[14] and Ziegler[20] on nonstoichiometric $Si_{1+y}Te_3$ *crystals* show that the close-packed layer structure of Si_2Te_3 exists over a broad range $\frac{1}{2} < y < 1$ of stoichiometries with dimers statistically missing from the Te octahedral cages. In the glasses the free energy of the layered cluster fragments is probably lowered even more than in the crystals as constraints due to long-range order are lifted, thus making feasible for the layered fragment to relax and accommodate an even wider range of cation to anion stoichiometries than is possible in the crystals. In our structural model of these glasses the drastic network reorganization taking place at the vector percolation threshold, $x=0.20$, can also be stimulated by a photon pump at $x \leq 0.20$, as revealed by our Raman scattering results discussed earlier in Sec. III C.

IV. CONCLUDING REMARKS

In summary, our scanning-calorimetry results and Raman and Mössbauer spectroscopic observations on Si_xTe_{1-x} glasses provide evidence of a major structural reorganization taking place at the vector percolation threshold. The proposed structural reorganization provides a natural explanation for several of our observations which include (a) the sharp decline in $\langle \Delta \rangle$ marked by a cusp at $x=0.20$ (1), (b) the absence of T_{c1} crystallization exotherm associated with Te chains at $x \geq 0.20$, (c) the formation of c-Si_2Te_3 as the final crystalline product upon crystallization of the Si-rich ($x > 0.20$) glasses, and (d) rapid growth in scattering strength of vibrational modes characteristic of microcrystalline-Si_2Te_3 at $x \geq 0.20$. Our structural model could provide a basis to understand the cusp near $x=0.20$ in the composition dependence of the semiconductor-metal transition pressure observed elsewhere.[21] The structural consequences of rigidity percolation in glassy networks appear to have a common theme. The present results on Si-Te glasses and those reported recently on Ge-Se (Ref. 3) and As-Ge-Se glasses[4] suggest that at or above the mechanical threshold, the elastically rigid domains largely derive from crystal-like molecular fragments.[22]

Previous observations of mechanical threshold anomalies in Ge_xSe_{1-x} alloy glasses have generally shown[3,5] weak power-law behavior proportional to $(x-x_c)^{\alpha}$ with α of order 2 or 3. This is quite different from the kink shown in Fig. 2, or the cusp in the metal-semiconductor transition pressure $P_t(x)$ reported by Asokan *et al.*,[21] both of which correspond to $\alpha < 1$. Why are the threshold anomalies so much stronger in Si_xTe_{1-x} than in Ge_xSe_{1-x}? We believe that the answer to this question is contained in the respective crystal structures of $Si_{1+y}Te_3$ and $GeSe_2$. It seems likely to us that the defect compound $Si_{1+y}Te_3$ is stabilized by internal pressure, and that at the mechanical threshold $x=x_c$ there is a kink in the internal pressure $P_i(x)$ which stabilizes $SiTe_3$-type defect submicrocrystallites. For stable crystals like $GeSe_2$ a glassy alloy Ge_xSe_{1-x} may be a partially phase-separated mixture of submicrocrystalline clusters of $Ge_{22}Se_{46}$ and Se chain segments near

$x = x_c = 0.2$. This produces threshold effects almost as weak as those predicted theoretically for an idealized (defect-free) continuous random-network model.[2]

It is striking that cluster stability (stoichiometrically stable crystals compared to stoichiometrically unstable defect crystals) has a drastic effect on α but very little effect on x_c. Moreover, that small effect is such as to bring x_c (within experimental resolution) exactly to the ideal theoretical value $x_c = 0.20$ for the defect case. It appears that nonequilibrium effects could be responsible for $x_c = 0.23$ (2) in Ge_xSe_{1-x} alloys.[5] These nonequilibrium effects on global mechanical equilibrium may be minimized by a nonequilibrium concentration of point defects which locally relieves global mechanical stresses generated by quenching.

ACKNOWLEDGMENTS

We thank Dr. S. Asokan and collaborators for sharing scanning calorimetry results on Si-Te glasses prior to their publication in Ref. 10. The work at University of Cincinnati was supported by Grant No. DMR-85-21005 from the National Science Foundation.

[1]J. C. Phillips, J. Non-Cryst. Solids **34**, 153 (1979); **43**, 37 (1981).

[2]M. Thorpe, J. Non-Cryst. Solids **57**, 355 (1983).

[3]R. Ota, T. Yamate, N. Soga, and M. Kunugi, J. Non-Cryst. Solids **29**, 67 (1978); J. Y. Duquesne and G. Bellessa, J. Phys. (Paris) C-10 **46**, 445 (1985).

[4]B. L. Halfpap and S. M. Lindsay, Phys. Rev. Lett. **57**, 847 (1986).

[5]W. Bresser, P. Boolchand, and P. Suranyi, Phys. Rev. Lett. **56**, 2493 (1986).

[6]K. Murase, T. Funkunaga, K. Yakushiji, T. Yoshimi, and I. Yunoki, J. Non-Cryst. Solids **59-60**, 883 (1983); also see P. M. Bridenbaugh, G. P. Espinosa, J. E. Griffiths, J. C. Phillips, and J. P. Remeika, Phys. Rev. B **20**, 4140 (1979).

[7]J. E. Griffiths, G. P. Espinosa, J. P. Remeika, and J. C. Phillips, Phys. Rev. B **25**, 1272 (1982).

[8]Jack Wells and P. Boolchand, J. Non-Cryst. Solids **89**, 31 (1987).

[9]J. Cornet, in *Structure and Properties of Non-Crystalline Semiconductors,* edited by B. T. Kolomiets (Academy of Sciences of the USSR, Leningrad, 1975), p. 72.

[10]S. Asokan, G. Parthasarathy, and E. S. R. Gopal, J. Non-Cryst. Solids **86**, 48 (1986).

[11]M. B. Meyers and E. J. Felty, Mater. Res. Bull. **2**, 535 (1967).

[12]J. Grothaus and P. Boolchand, J. Non-Cryst. Solids **72**, 1 (1985).

[13]A. S. Pine and G. Dresselhaus, Phys. Rev. B **4**, 356 (1971); also see M. H. Brodsky, R. J. Gambino, J. E. Smith, and Y. Yacoby, Phys. Status Solidi B **52**, 609 (1972).

[14]P. E. Gregoriades, G. L. Bleris, and J. Stoemenos, Acta Crystallogr. Sect. B **39**, 421 (1983), and references therein.

[15]J. E. Griffiths, M. Malyj, G. P. Espinosa, and J. P. Remeika, Phys. Rev. B **30**, 6978 (1984).

[16]M. Tenhover, M. A. Hazzle, and R. K. Grasselli, Phys. Rev. Lett. **51**, 404 (1983).

[17]M. Malyj, G. P. Espinosa, and J. E. Griffiths, Phys. Rev. B **31**, 3672 (1985).

[18]P. Boolchand, in *Physical Properties of Amorphous Materials,* edited by David Adler, Brian B. Swartz, and Martin C. Steele (Plenum, New York, 1985), p. 221.

[19]P. Boolchand, B. B. Triplett, S. S. Hanna, and J. P. deNeufville, in *Mossbauer Effect Methodology,* edited by I. J. Gruverman, Carl W. Seidel, and David K. Dieterly (Plenum, New York, 1974), Vol. 9, p. 53.

[20]K. Ziegler, H. Junker, and V. Birkholz, Phys. Status Solidi A **37**, K97 (1976).

[21]S. Asokan, G. Parthasarathy, and E. S. R. Gopal, in Proceedings of XIV International Congress on Glass, 1986 (unpublished), and also see *Key Engineering Materials,* Proceedings of the International Conference on Metallic and Semiconducting Glasses, Hyderabad, India, 1986, edited by Anil K. Bhatnagar (Transtech, Switzerland, 1987), Vol. 13, p. 119.

[22]P. Boolchand, Phys. Rev. Lett. **57**, 3233 (1986). And also see P. Boolchand, in *Key Engineering Materials,* Proceedings of the International Conference on Metallic and Semiconducting Glasses, Hyderabad, India, 1986, edited by Anil K. Bhatnagar (Transtech, Switzerland, 1987), Vol. 13, p. 131.